

## **Supplementary Material for the paper**

### **Heterogeneous chemistry of monocarboxylic acids on $\alpha\text{-Al}_2\text{O}_3$ at different relative humidities**

By:

S. R. Tong, L. Y. Wu, M. F. Ge, W. G. Wang, and Z. F. Pu

Correspondence to: M. F. Ge (gemaofa@iccas.ac.cn)

**Table S1.** Assignment of the vibrational frequencies ( $\text{cm}^{-1}$ ) for adsorbed carboxylates following exposure of  $\alpha\text{-Al}_2\text{O}_3$  particles surfaces to carboxylic acids.

Surface species	Absorbance bands	Vibrational mode assignment
Adsorbed formate species <sup>a</sup>		
	1378	C–H in plane bend
	1393	OCO symmetric stretch
	1600	OCO antisymmetric stretch
	2750	OCO symmetric stretch and C–H in plane bend
	2866	C–H stretch
	2985	OCO symmetric stretch and C–H in plane bend
Adsorbed acetate species <sup>b</sup>		
	1343	symmetric bend of $\text{CH}_3$
	1424	deformation mode of $\text{CH}_3$
	1468	OCO symmetric stretch
	1578	OCO antisymmetric stretch
	2935	$\text{CH}_3$ symmetric stretch
	2986	C–H antisymmetric stretch
	3016	C–H antisymmetric stretch
Adsorbed propionate species <sup>c</sup>		
	1259	out-of-phase twisting of $\text{CH}_2$
	1303	in-plane wagging mode of $\text{CH}_2$
	1382	symmetric deformation of $\text{CH}_3$
	1420	asymmetric bending of $\text{CH}_3$ and OCO symmetric stretch
	1475	antisymmetric deformation of $\text{CH}_3$ , scissoring modes of $\text{CH}_2$ , and OCO symmetric stretch
	1566	OCO antisymmetric stretch
	2887	C–H symmetric stretch of $\text{CH}_2$
	2946	C–H symmetric stretch of $\text{CH}_3$
	2980	C–H antisymmetric stretch of $\text{CH}_2$

<sup>a</sup> from Chauvin et al. (1990), Amenomiya (1979), and Walmsley et al. (1981).

<sup>b</sup> from Chen and Bruce (1995) and Walmsley et al. (1981).

<sup>c</sup> from Yang et al. (2006), Kakihana and Akiyama (1987), and Yuzawa et al. (1997).

**Table S2.** Structural parameters and vibration frequencies (in  $\text{cm}^{-1}$ ) for the calculated model formates I-III, calculated at B3LYP/6-311++G(3df,3pd) level of theory.

Mode	Optimized structural parameters					Vibrational mode		
	Bond length ( $\text{\AA}$ )			Angle (degrees)		Calculated frequencies ( $\text{cm}^{-1}$ )		
	C-O1	C-O2	Al1-O2	O1-C-O2	Al1-O2-C	$\delta(\text{CH})$	$\nu_s(\text{OCO})$	$\nu_{as}(\text{OCO})$
Monodentate	1.22	1.31	1.78	125.8	126.0	1405	1304	1698
						(1367) <sup>a</sup>	(1268) <sup>a</sup>	(1651) <sup>a</sup>
Bidentate	1.27	1.27	1.89	116.8	86.1	1296	1400	1556
						(1260) <sup>a</sup>	(1362) <sup>a</sup>	(1513) <sup>a</sup>
Bridging	1.25	1.26	1.86	126.6	134.0	1422	1432	1651
						(1383) <sup>a</sup>	(1393) <sup>a</sup>	(1606) <sup>a</sup>

<sup>a</sup> Scaled calculated frequencies.

**Table S3.** Structural parameters and vibration frequencies (in  $\text{cm}^{-1}$ ) for the calculated model acetates I-III, calculated at B3LYP/6-311++G(3df,3pd) level of theory.

Mode	Optimized structural parameters					Vibrational mode		
	Bond length ( $\text{\AA}$ )		Angle (degrees)			Calculated frequencies ( $\text{cm}^{-1}$ )		
	C-O1	C-O2	A11-O2	O1-C-O2	A11-O2-C	$\delta(\text{CH})$	$\nu_s(\text{OCO})$	$\nu_{\text{as}}(\text{OCO})$
Monodentate	1.23	1.32	1.78	123.4	126.6	1410 (1371) <sup>a</sup>	1344 (1307) <sup>a</sup>	1690 (1644) <sup>a</sup>
Bidentate	1.28	1.28	1.91	114.9	87.1	1444 (1404) <sup>a</sup>	1468 (1428) <sup>a</sup>	1529 (1487) <sup>a</sup>
Bridging	1.26	1.26	1.84	124.0	131.2	1470 (1430) <sup>a</sup>	1513 (1472) <sup>a</sup>	1616 (1572) <sup>a</sup>

<sup>a</sup> Scaled calculated frequencies.

**Table S4.** Structural parameters and vibration frequencies (in  $\text{cm}^{-1}$ ) for the calculated model propionates I-III, calculated at B3LYP/6-311++G(3df,3pd) level of theory.

Mode	Optimized structural parameters					Vibrational mode		
	Bond length ( $\text{\AA}$ )		Angle (degrees)			Calculated frequencies ( $\text{cm}^{-1}$ )		
	C-O1	C-O2	A11-O2	O1-C-O2	A11-O2-C	$\delta(\text{CH}_3)+$ $\nu_s(\text{OCO})$	$\delta(\text{CH}_3)+$ $\nu_s(\text{OCO})$	$\nu_{\text{as}}(\text{OCO})$
Monodentate	1.23	1.32	1.77	123.3	126.5	1284 (1249) <sup>a</sup>	1408 (1369) <sup>a</sup>	1686 (1640) <sup>a</sup>
Bidentate	1.28	1.28	1.87	114.7	87.1	1449 (1409) <sup>a</sup>	1525 (1483) <sup>a</sup>	1508 (1467) <sup>a</sup>
Bridging	1.27	1.26	1.84	123.8	135.7	1493 (1452) <sup>a</sup>	1514 (1473) <sup>a</sup>	1608 (1564) <sup>a</sup>

<sup>a</sup> Scaled calculated frequencies.

Table S5 Summary of kinetic results from the reaction HCOOH and  $\alpha$ -Al<sub>2</sub>O<sub>3</sub>

No.	[HCOOH] <sup>a</sup>	R <sup>b</sup>	R{HCOO <sup>-</sup> } <sup>c</sup>
1	0.77	0.0024	0.10
2	1.54	0.0047	0.20
3	2.46	0.0087	0.37
4	6.15	0.022	0.99
5	8.20	0.032	1.39
6	12.3	0.048	2.08
7	16.4	0.055	2.38
8	24.6	0.092	3.96

<sup>a</sup> In units of 10<sup>13</sup> molecules cm<sup>-3</sup>;<sup>b</sup> Observed rate (integrated absorbance units min<sup>-1</sup>) of formate formation obtained from the integrated area of all absorptions in the region 1250-1450 cm<sup>-1</sup>.<sup>c</sup> Rate of formate in 10<sup>15</sup> ions s<sup>-1</sup> calculated from the integrated infrared absorption in the region 1250-1450 cm<sup>-1</sup> the calibrated by ion chromatography analysis of the formate as described in the text.

Table S6 Summary of kinetic results from the reaction CH<sub>3</sub>COOH and  $\alpha$ -Al<sub>2</sub>O<sub>3</sub>

No.	[CH <sub>3</sub> COOH] <sup>a</sup>	R <sup>b</sup>	R{CH <sub>3</sub> COO <sup>-</sup> } <sup>c</sup>
1	0.77	0.0057	0.28
2	1.54	0.0098	0.48
3	2.46	0.015	0.74
4	3.08	0.020	0.98
5	4.67	0.033	1.60
6	6.15	0.035	1.70
7	12.3	0.073	3.56
8	24.6	0.150	7.49

<sup>a</sup> In units of 10<sup>13</sup> molecules cm<sup>-3</sup>;<sup>b</sup> Observed rate (integrated absorbance units min<sup>-1</sup>) of acetate formation obtained from the integrated area of all absorptions in the region 1360-1510 cm<sup>-1</sup>.<sup>c</sup> Rate of acetate in 10<sup>15</sup> ions s<sup>-1</sup> calculated from the integrated infrared absorption in the region 1360-1510 cm<sup>-1</sup> the calibrated by ion chromatography analysis of the acetate as described in the text.

Table S7 Summary of kinetic results from the reaction CH<sub>3</sub>CH<sub>2</sub>COOH and  $\alpha$ -Al<sub>2</sub>O<sub>3</sub>

No.	[CH <sub>3</sub> CH <sub>2</sub> COOH] <sup>a</sup>	R <sup>b</sup>	R{CH <sub>3</sub> CH <sub>2</sub> COO <sup>-</sup> } <sup>c</sup>
1	0.51	0.0014	0.072
2	1.03	0.0031	0.16
3	1.64	0.0044	0.23
4	2.95	0.0078	0.41
5	4.1	0.012	0.62
6	8.2	0.028	1.45
7	12.3	0.042	2.19
8	16.4	0.067	3.47

<sup>a</sup> In units of 10<sup>13</sup> molecules cm<sup>-3</sup>;

<sup>b</sup> Observed rate (integrated absorbance units min<sup>-1</sup>) of propionate formation obtained from the integrated area of all absorptions in the region 1330-1510 cm<sup>-1</sup>.

<sup>c</sup> Rate of propionate in 10<sup>15</sup> ions s<sup>-1</sup> calculated from the integrated infrared absorption in the region 1330-1510 cm<sup>-1</sup> the calibrated by ion chromatography analysis of the propionate as described in the text.

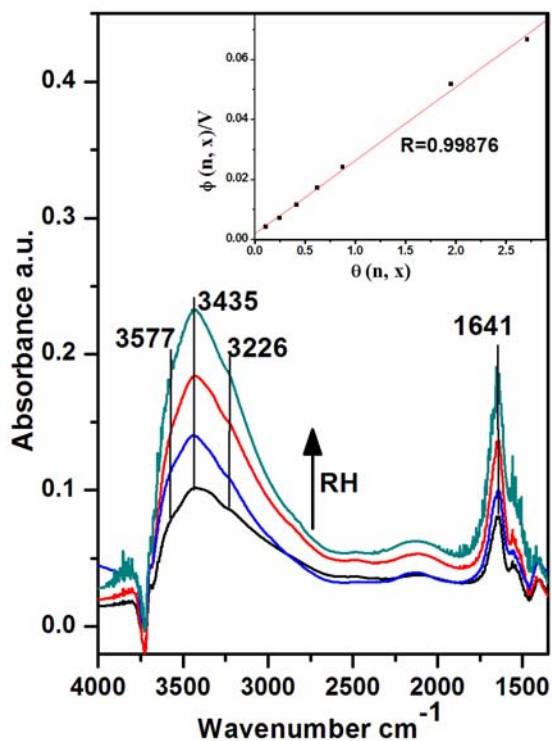


Figure S1 Absorption spectra for water vapour adsorption on dry  $\alpha$ -Al<sub>2</sub>O<sub>3</sub> powder at 300 K as a function of relative humidity 10%, 30%, 60%, and 80%, respectively. Each spectrum was referenced to the appropriate clean oxide spectrum prior to exposure to water vapour. The insets show the linearized BET fits for water adsorption on  $\alpha$ -Al<sub>2</sub>O<sub>3</sub> using the integrated absorbance of the OH stretch in 3000-3800 cm<sup>-1</sup> region.